

Nanowire of hexagonal gallium oxynitride: Direct observation of its stacking disorder and its long nanowire growth

Yuji Masubuchi^{a,*}, Ryohei Yamaoka^a, Tetsuya Tohei^b, Teruyasu Mizoguchi^c,
Yuichi Ikuhara^b, Shinichi Kikkawa^a

^a Faculty of Engineering, Hokkaido University, N13 W8, Kita-ku, Sapporo, Hokkaido 060-8628, Japan

^b Institute of Engineering Innovation, The University of Tokyo, 2-11-16, Yayoi, Bunkyo-ku, Tokyo 113-8656, Japan

^c Institute of Industrial Science, The University of Tokyo, 4-6-1, Komaba, Meguro-ku, Tokyo 153-8505, Japan

Available online 12 November 2011

Abstract

The crystal structure of gallium oxynitride nanowire was investigated by using scanning transmission electron microscopy. Gallium oxynitride nanowire was directly observed to have a biphasic wurtzite and zinc-blende structure. There was a stacking disorder of several atomic layers between the two phases. The new biphasic nanowire formed due to the presence of Ni in starting material because its nitride has a zinc-blende structure whereas gallium oxynitride has the wurtzite structure. Crystal growth of gallium oxynitride nanowires was studied using seed crystals. Seed crystals and amorphous gallium oxide precursors were annealed under different ammonia flow rates to grow gallium oxynitride nanowires. The nanowires grew to length of 150 μm but they did not grow laterally when the ammonia flow rate was 50 mL/min.

© 2011 Elsevier Ltd. All rights reserved.

Keywords: Fibres; Electron microscopy; Oxynitrides; Defects

1. Introduction

Gallium nitride (GaN) and the related materials have been widely studied for various applications including UV-blue light emitting diodes, laser diodes and UV detectors.^{1–3} Their nanowires have been attracting interest for a wide range of optical and electronic applications, such as UV lasers, field effect transistors and logic gates.^{4–6} Nanowires can be grown by various methods, including chemical vapor deposition (CVD), metalorganic CVD and vapor phase epitaxy using Au, Ni, Co or Si as catalysts for vapor–liquid–solid (VLS) growth.^{7–10} Nanotubes and nanobelts of GaN have been also prepared by nitridation of $\beta\text{-Ga}_2\text{O}_3$ by NH_3 .^{11,12}

Theoretical calculations predicted that spinel type gallium oxynitride $\gamma\text{-Ga}_3\text{O}_3\text{N}$ will form from monoclinic $\beta\text{-Ga}_2\text{O}_3$ and wurtzite GaN under high pressure and that the oxynitride will be stabilized by introducing gallium vacancies.^{13,14} Gallium

oxynitride (GaON) with a wurtzite-like structure was first prepared by ammonolysis of NiGa_2O_4 .¹⁵ Its crystal structure has been expected to be 6H polytypoid, because its Raman spectrum showed characteristics for both wurtzite (2H) and zinc-blende (3C).¹⁶ Wurtzite-type GaON with a chemical composition of $(\text{Ga}_{0.89}\square_{0.11})(\text{N}_{0.66}\text{O}_{0.34})$ was also prepared by ammonolysis of amorphous gallium oxide obtained through the citrate route,¹⁷ where the symbol \square indicates a gallium site vacancy. It is expected to have a non-stoichiometric nitrogen/oxygen ratio and to contain gallium site vacancies. It is not clear whether it has a fixed chemical composition or the GaN analogue partially substituted with oxide ions. Some kinds of 3d transition metals were doped into the GaON to study the magnetic properties by using similar preparation methods.^{18–21} Ammonolysis of an amorphous gallium oxide precursor containing a few percent of Ni or Co additives produced GaON nanowires mixed with agglomerated GaON grains.²² The nanowires grew to length of several micrometers and widths of several tens of nanometers at an ammonolysis temperature of 750 °C. Their electron diffraction pattern indicates that they grew parallel to the hexagonal *c*-plane. Ni or Co additives were found in the agglomerated

* Corresponding author. Tel.: +81 011 706 6742; fax: +81 011 706 6740.
E-mail address: yuji-mas@eng.hokudai.ac.jp (Y. Masubuchi).

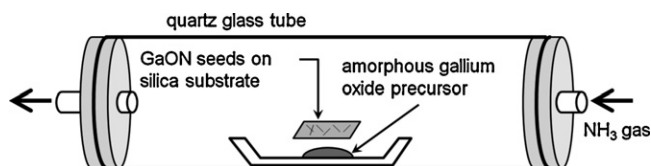


Fig. 1. Schematic diagram of the nanowire growth. GaON seed crystals on silica substrate were placed in a quartz glass tube furnace with an amorphous gallium oxide precursor.

grains, but not in the GaON nanowires. The GaON nanowires were assumed to be grown by the catalytic behavior of Ni or Co, which precipitated during ammonolysis due to the instability of their nitrides.²³ One-dimensional growth occurred because metal precipitates obstruct isotropic two-dimensional growth of GaON in the hexagonal *c*-plane. The nanowires did not grow by VLS growth. They should be single crystals with a fixed chemical composition. They are expected to have a highly disordered wurtzite (2H) crystal structure with some zinc-blende (3C) type stacking disorders based on X-ray diffraction (XRD) patterns of the mixture of nanowires and agglomerated GaON grains. Such structural characteristics can be observed directly in single crystalline products. However, there have been no direct microscopic observations of the stacking disorder in GaON.

The optical and electronic transport properties of the nanowires can be controlled by controlling their crystal structure and chemical composition. Crystal growth along the above-mentioned biphasic wurtzite and zinc-blende structure is required to their characterizations and applications in optical, transport properties and so on. Crystal growth by using seed crystals has not yet been investigated. The presence of stacking disorder as well as growth conditions may affect the nanowire morphology.

In this study, the atomic scale observation of the GaON nanowire was carried out by using scanning transmission electron microscopy (STEM) technique to clarify their crystal structure. Crystal growth of GaON nanowires was also studied by using seed crystals separated from the agglomerated product obtained by ammonolysis of an amorphous gallium oxide precursor containing 3 at.% Ni additives. The effect of varying the ammonia flow rate on their morphology was investigated.

2. Experimental

A mixture of GaON seed crystals and agglomerated GaON grains was prepared by ammonolysis of an amorphous gallium oxide precursor containing 3 at.% Ni. The starting materials were gallium nitrate hydrate $\text{Ga}(\text{NO}_3)_3 \cdot 9\text{H}_2\text{O}$ and nickel nitrate hydrate $\text{Ni}(\text{NO}_3)_2 \cdot 6\text{H}_2\text{O}$ purchased from Wako Pure Chemicals with 3N purity. These reagents were dissolved in distilled water containing citric acid (Wako Pure Chemicals with 3N purity). The solution condensed to form a gel on a hot plate under stirring. The gel was calcined in air at 350 °C for 1 h to obtain an amorphous oxide precursor. It was then nitrided at 750 °C for 10 h in an ammonia flow of 50 mL/min. The nitrided product contained GaON nanowires and agglomerated grains. To separate the nanowires so that they could be used as seed

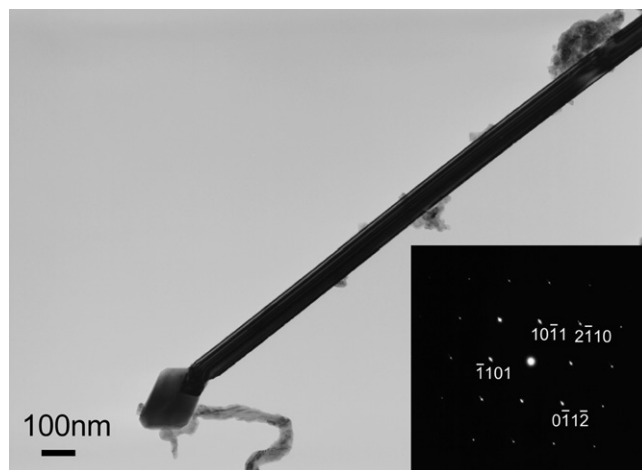


Fig. 2. TEM image and (inset) electron diffraction pattern of GaON nanowire prepared by ammonolysis of amorphous gallium oxide precursor with 3 at.% Ni at 750 °C under NH₃ flow rate of 50 mL/min.

crystals for subsequent crystal growth, the nitrided product was ultrasonically separated in acetone and the supernatant solution was dropped onto a silica substrate. The silica substrate was then placed in a tube furnace for the crystal growth with the gallium oxide precursor which had been prepared through above-mentioned process without Ni additives. Fig. 1 shows a schematic diagram of the crystal growth setup. The seed crystal and the precursor were annealed at 750 °C for 10 h under NH₃ flow rates of 20–100 mL/min.

XRD patterns were collected using a diffractometer with Cu K α radiation (Ultima IV, Rigaku). The microstructure of the products on carbon tapes was observed by scanning electron microscopy (SEM) (JSM-6390LV, JEOL). Transmission electron microscopy (TEM) samples were prepared by suspending the nanowires, which was obtained by ammonolysis of amorphous gallium oxide at 750 °C under NH₃ flow rate of 50 mL/min with 3 at.% of Ni additives, in ethanol and then supporting them on a micro-grid coated copper mesh. TEM and STEM observations were performed using JEM-2010HC (JEOL) and JEM-2100F (JEOL) equipped with a Cs-corrector (CEOS GmbH). Elemental analysis was performed by STEM energy-dispersive X-ray spectroscopy (EDX) (HD-2000, Hitachi).

3. Results and discussion

3.1. Direct observation of stacking disorder in GaON nanowires

Fig. 2 shows a TEM image of a GaON nanowire prepared by ammonolysis of amorphous gallium oxide at 750 °C under NH₃ flow rate of 50 mL/min with 3 at.% of Ni additives. It is several micrometers long and about 100 nm wide. Its electron diffraction pattern was indexed with a hexagonal lattice and its growth direction was parallel to the hexagonal *c*-plane, as reported in a previous study.²² A streak in the electron diffraction pattern suggests the presence of stacking disorder along the *c*-axis. Fig. 3(a) shows a bright-field (BF) STEM image of a

gallium site must be vacant.¹⁷ Gallium vacancies and incorporated oxide ions may introduce stacking disorder into the GaON lattice. α -Ga₂O₃ crystallizes in the corundum structure in which one third of the octahedral sites are vacant in hcp.²⁵ GaN has the wurtzite structure in hcp and β -Ga₂O₃ crystallizes in the ccp with partially occupied tetrahedral and octahedral sites.^{26,27} The different stacking in simple gallium compounds may suggest understanding of the complicated stacking in relation to the gallium vacancy. Polytypoid structure, which corresponds to wurtzite-type AlN with a different stacking sequence, has been observed in aluminum oxynitrides and SiAlON with a cation-deficient composition (i.e., $M/X < 1$).^{28,29} Incorporated oxide ions and gallium vacancies may stabilize the biphasic wurtzite and zinc-blende structure with stacking disorders.

3.2. Crystal growth of GaON nanowires on seed crystal

Seed crystals separated on the silica substrate were annealed with amorphous gallium oxide at 750 °C under flowing NH₃ to achieve homogeneous crystal growth and to obtain larger GaON nanowires. Fig. 4 shows SEM images of GaON nanowires grown under four different NH₃ flow rates. Nanowires did not grow under similar conditions when silica substrates without seed crystals were used. Many short (i.e., <10 μ m), twisty GaON nanowires were obtained under a NH₃ flow rate of 20 mL/min (Fig. 4(a)). GaON nanowires that were more than 100 μ m long and short, twisty nanowires were observed for annealing under a NH₃ flow rate of 30 mL/min (Fig. 4(b)). The number of short, twisty nanowires decreased when the NH₃ flow rate was increased to 50 mL/min (Fig. 4(c)). In the product, very long nanowires that were over 100 μ m long were formed with several branches in every several tens of micrometers. However, the nanowires did not undergo crystal growth at a NH₃ flow rate of 100 mL/min as indicated by the fact that the small grains and very short nanowires in Fig. 4(d) have similar distributions to those observed before annealing. During crystal growth of GaN, gallium vapor phase such as Ga₂O are supplied from the β -Ga₂O₃ precursor under flowing NH₃.³⁰ The NH₃ flow rate of 100 mL/min was too fast to supply gallium vapor phase for crystal growth. On the other hand, a low NH₃ flow rate may allow the vapor phase to stay near the seed crystal in a longer duration, resulting in an excess supply of gallium vapor phase on the seed. This excess supply may favor GaON nucleation on the substrate surface rather than crystal growth of the seed crystals.

Fig. 5 shows histograms for the nanowire width and length observed on the products obtained at the three NH₃ flow rates. There is little difference between the width distributions of the products. The GaON nanowire width after crystal growth did not change significantly on changing the NH₃ flow rate. The GaON nanowires were significantly elongated at a NH₃ flow rate of 50 mL/min and reached a maximum length of 150 μ m. While a low flow rate of 20 mL/min was not effective for growing the nanowires, it increased the number of GaON nanowires because of increased nucleation. The stacking disorders parallel to the hexagonal *c*-plane in GaON may obstruct crystal growth

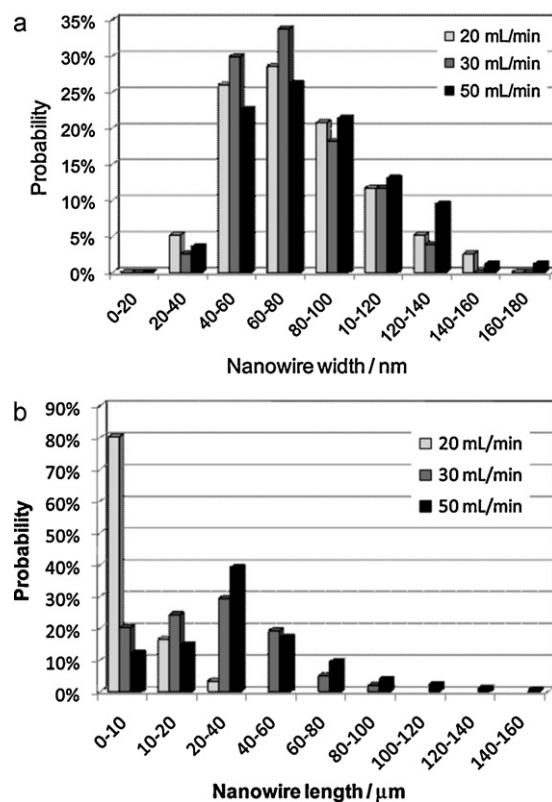


Fig. 5. (a) Width and (b) length histograms of GaON nanowires grown at different NH₃ flow rates.

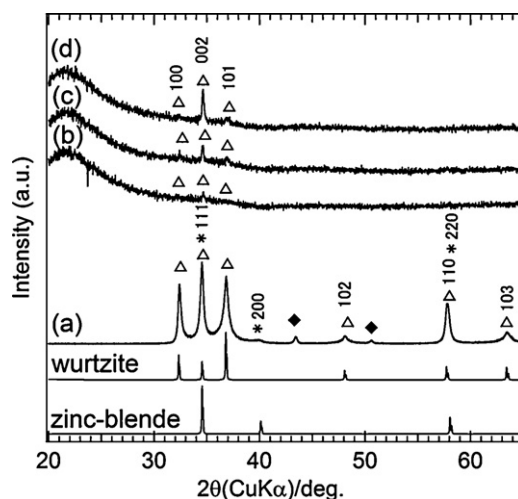


Fig. 6. XRD patterns of gallium oxynitride nanowires grown at 750 °C under NH₃ flow rates of (b) 20, (c) 30, and (d) 50 mL/min measured on a silica substrate. (a) Reference XRD pattern of gallium oxynitride powder prepared by ammonolysis of Ga–Ni oxide precursor, containing nanowires and agglomerated grains. Simulated XRD patterns for a chemical composition (Ga_{0.89}□_{0.11})(N_{0.66}O_{0.34}) with the hexagonal wurtzite structure ($a=0.3189$ nm and $c=0.5181$ nm¹⁷) and with the cubic zinc-blende structure ($a=0.4486$ nm) are also shown at the bottom. Open triangles indicate diffraction peaks for the wurtzite lattice. Peaks with asterisks are also assigned to a zinc-blend lattice. Filled diamonds indicate diffraction peaks of GaNi₃C_{0.5}.

perpendicular to the hexagonal *c*-plane and enhance it parallel to the *c*-plane.

XRD patterns of the as-grown nanowires are shown in Fig. 6(b–d) and Fig. 6(a) shows the XRD pattern for a mixture of GaON nanowires and agglomerated grains prepared by ammonolysis of the gallium oxide precursor at 750 °C with 3 at.% of Ni additives. GaON prepared with Ni additives crystallizes with the biphasic wurtzite and zinc-blende structure with stacking disorders (Fig. 3). Fig. 6(b–d) shows remarkable preferred orientation. Their hexagonal *c*-plane was parallel to the silica substrate because the nanowires grown in the *c*-plane readily lie on the silica substrate. Their optical and electrical properties are currently being investigated.

4. Conclusion

The atomic-scale microstructure of gallium oxynitride nanowires prepared by ammonolysis of a Ga–Ni oxide precursor was observed by STEM. The gallium oxynitride nanowires consisted of wurtzite and zinc-blende lattices with stacking disorder of several atomic layers in between. The nanowires grew parallel to the hexagonal *c*-plane and the cubic (1 1 1) plane. Gallium oxynitride nanowires were grown to a length of 150 μm using short seed crystals at 750 °C under 50 mL/min ammonia flow.

Acknowledgments

This research was partly supported by Grant-in-Aid for Scientific Research on Priority Areas (No. 19053001 and 22015001) from the Ministry of Education, Culture, Sports, Science and Technology (MEXT) of Japan and for Exploratory Research (No. 236551388) from the Japan Society for the Promotion of Science (JSPS). Y.M. acknowledges financial support from the Global COE Program (Project No. B01: “Catalysis as the Basis for Innovation in Materials Science”) from MEXT of Japan. A part of this work was conducted in the Center for Nano Lithography & Analysis, The University of Tokyo, supported by MEXT, Japan.

References

1. Nakamura S, Mukai T, Senoh M. *Appl Phys Lett* 1994;**64**:1687–9.
2. Nakamura S, Senoh M, Nagahama S, Jwasa N, Tamada T, Matsushita T, Kiyoku H, Sugimoto Y. *Jpn J Appl Phys* 1996;**35**:L74–6.

3. Akasaki I, Amano H, Kito M, Hiramatsu K. *J Lumin* 1991;**48**:666–70.
4. Johnson JC, Choi HJ, Knutsen KP, Schaller RD, Yang P, Saykally RJ. *Nat Mater* 2002;**1**:106–10.
5. Huang Y, Duan X, Cui Y, Lieber CM. *Nano Lett* 2002;**2**:101–4.
6. Huang Y, Duan X, Cui Y, Lauhon LJ, Kim KH, Lieber CM. *Science* 2001;**294**:1313–7.
7. Lee SK, Choi HJ, Pauzauskie P, Yang P, Cho NK, Park HD, Suh EK, Lim KY, Lee HJ. *Phys Status Solidi B* 2004;**241**:2775–8.
8. Byeun YK, Han KS, Choi SC. *J Electroceram* 2006;**17**:903–7.
9. Qin LX, Xue CS, Zhuang HZ, Yang ZZ, Li H, Chen JH, Wang Y. *Appl Phys A: Mater Sci Process* 2008;**91**:675–8.
10. Kwon HY, Shin MJ, Choi YJ, Moon JY, Ahn HS, Yi SN, Kim S, Ha DH, Park SH. *J Cryst Growth* 2009;**311**:4146–51.
11. Luo LQ, Yu K, Zhu ZQ, Zhang YS, Ma HL, Xue CS, Yang YG, Chen SQ. *Mater Lett* 2004;**58**:2893–6.
12. Dinesh J, Eswaramoorthy M, Rao CNR. *J Phys Chem C* 2007;**111**:510–3.
13. Kroll P, Dronskowski R, Martin M. *J Mater Chem* 2005;**15**:3296–302.
14. Martin M, Dronskowski R, Janek J, Becker KD, Roehrens D, Brendt J, Lumey MW, Nagarajan L, Valov I, Borger A. *Prog Solid State Chem* 2009;**37**:132–52.
15. Kerlau M, Merdignac-Conanec O, Reichel P, Barsan N, Weimar U. *Sens Actuators B* 2006;**115**:4–11.
16. Cailleaux X, Lucas MCM, Merdignac-Conanec O, Tessier F, Nagasaka K, Kikkawa S. *J Phys D: Appl Phys* 2009;**42**:045408-1–6.
17. Kikkawa S, Nagasaka K, Takeda T, Bailey M, Sakurai T, Miyamoto Y. *J Solid State Chem* 2007;**180**:1984–9.
18. Kikkawa S, Ohtaki S, Takeda T, Yoshiasa A, Sakurai T, Miyamoto Y. *J Alloys Compd* 2008;**450**:152–6.
19. Yamamoto S, Kikkawa S, Masubuchi Y, Takeda T, Wolff H, Dronskowski R, Yoshiasa A. *Solid State Commun* 2008;**147**:41–5.
20. Yamamoto S, Kikkawa S, Masubuchi Y, Takeda T, Okube M, Yoshiasa A, Lumey M, Dronskowski R. *Mater Res Bull* 2009;**44**:1656–9.
21. Miyaake A, Masubuchi Y, Takeda T, Kikkawa S. *Mater Res Bull* 2010;**45**:505–8.
22. Miiyaake A, Masubuchi Y, Takeda T, Motohashi T, Kikkawa S. *Dalton Trans* 2010;**39**:6106–11.
23. Eck B, Dronskowski R, Takahashi M, Kikkawa S. *J Mater Chem* 1999;**9**:1527–37.
24. Pennycook SJ, Rafferty B, Nellist PD. *Microsc Microanal* 2000;**6**:343–52.
25. Marezio M, Remeika JP. *J Chem Phys* 1967;**46**:1862–5.
26. Kamler G, Zachara J, Podsiadlo S, Adamowicz L, Gebicki W. *J Cryst Growth* 2000;**212**:39–48.
27. Geller S. *J Chem Phys* 1960;**33**:676–84.
28. Corbin ND. *J Eur Ceram Soc* 1989;**5**:143–54.
29. Thompson DP. In: Riely FL, editor. *Nitrogen Ceramics*. 1977. p. 129–35.
30. Kiyono H, Sakai T, Takahashi M, Shimada S. *J Cryst Growth* 2010;**312**:2823–7.